# Bake Stability of CdTe and ZnS on HgCdTe: An X-Ray Photoelectron Spectroscopy Study

S.K. JHA,[1] P. SRIVASTAVA,[1,5] R. PAL,[2] ANJALI,[1] H.K. SEHGAL,[1]
HEE CHUL LEE,[3] O.P. AGNIHOTRI,[3] and B.B. GONG[4]

1.—Semiconductor Engineering Laboratory, Department of Physics, IIT Delhi, New Delhi, India. 2.—Solid State Physics Laboratory, Timarpur, Delhi, India. 3.—Department of Electrical Engineering and Computer Science, Korea Advanced Institute of Science and Technology, Republic of Korea. 4.—Surface Science Centre, University of New Southwales, Sydney, Australia. 5.—E-mail: pankajs@physics.iitd.ernet.in

Mercury cadmium telluride ($Hg_{1-x}Cd_xTe$ or MCT) has been commonly used in devices for infrared (IR) detection. For the optimum performance of the device, a compatible surface-passivation technology that provides long-term stability is required. Using x-ray photoelectron spectroscopy (XPS), the present study examines the effects on $Hg_{0.8}Cd_{0.2}Te$ passivated with CdTe and ZnS undergoing baking in vacuum at temperatures typically used for dewar bakeout. Spectra recorded as a function of depth in both cases clearly show out-diffusion of Hg from the substrate toward the surface, even before the bakeout. On baking in vacuum, dramatic changes are observed in the ZnS/MCT case with complete loss of Hg from the sample up to the tested depth of more than 1,000 Å. Compositions of the HgCdTe matrix, formed after Hg out-diffusion, before and after the bakeout are also calculated at selected depths (from 250 Å to 700 Å), which is vital information from a device point of view, as it affects the bandgap of this narrow-band semiconductor.

**Key words:** XPS, depth profiling, HgCdTe, passivation

## INTRODUCTION

Mercury cadmium telluride ($Hg_{1-x}Cd_xTe$ or MCT) is a ternary compound whose composition x and, hence, bandgap can be tuned. This enables one to access the atmospheric-transmission windows between 3–5-µm and 8–14-µm wavelengths.[1] The surface states on this narrow-bandgap semiconductor dominate the electrical response, and therefore, it is essential that surface passivation be carried out before MCT can be incorporated into devices for infrared (IR) detection. A number of passivation layers grown by various methods have been studied and used for HgCdTe-detector fabrication.[2,3] As the next generations of IR devices are based on the monolithic IR focal-plane arrays, which have metal-insulator-semiconductor (MIS) structures for signal processing, it is of vital importance to know and tailor the properties of the interface between the insulating-passivating layer and the MCT. Moreover, one of the very important issues regarding these passivating layers is thermal stability of the passivant/MCT interface, as low-temperature thermal baking is an essential step of device packaging.

In the present work, we have examined bake stability of thermally evaporated ZnS and CdTe layers on MCT. Zinc sulfide is the first insulator that was used for the fabrication and study of MIS structures.[4] It has been used as a single layer and also in combination with other passivants. Although ZnS passivation has been reported to yield high performance, particularly in the case of medium-wave IR-HgCdTe detectors, its thermal stability has been a matter of concern.[5] Studies addressing some aspects of CdTe passivation have been reported.[2,6,7] The CdTe is considered to be better passivant than ZnS in the case of long-wave IR-HgCdTe devices, but efforts are still being made to tailor a desirable and thermally stable interface.[8,9] It has been reported[7] that thermal annealing removes the problem of the defective interface between CdTe and MCT. This was ascribed to

---

(Received October 29, 2002; accepted March 7, 2003)

interdiffusion of CdTe in a MCT matrix, which introduced compositional grading near the interface. This results in shifting of the "initial" defective interface in a relatively wider gap region. Recently, a HgCdTe p-n diode junction was passivated by compositionally graded HgCdTe formed by annealing in a Cd/Hg atmosphere.[10] It has been reported that the compositionally graded layer results in one order of magnitude higher $R_dA$ values than the one passivated by thermally deposited, unannealed CdTe. An underlying issue involved here is that one needs to build and maintain the right kind of physical and chemical constitution of the surface layer to control the resulting photo-electrical interface characteristics. To make these observations really useful from the device point of view, one has to know the concentration of various constituents (i.e., Hg, Cd, and Te) along the depth of the sample in various annealing conditions. To the best of our knowledge, a detailed quantitative study exclusively focusing on properties of the interfaces of ZnS/MCT and CdTe/MCT and examining their bake stability is not available in the literature. We have used x-ray photoelectron spectroscopy (XPS) for this purpose. To examine the chemical states of various elements and composition at different depths, core-level spectra of various constituents have been recorded and analyzed.

## EXPERIMENTAL DETAILS

For the present investigations, p-type $Hg_{0.8}Cd_{0.2}Te$/CdZnTe epilayer (Fermionics, Simi Valley, CA) were used. The CdTe and ZnS layers were deposited by thermal-evaporation technique. The thickness of these layers was kept 200 Å. It may be mentioned here that film thickness of 200 Å is much lower than the passivation-layer thickness used for device fabrication. Thicker layers could not be used for this study because of practical difficulties involved in depth profiling. Sustained-sputter etching through the thicker layers could have resulted in the perturbation of the interfacial composition itself. Therefore, a thinner passivation layer was used to maintain as close to the actual interfacial composition as possible and to study this region with a higher resolution. Effects of baking on the interfacial region may still be close to the real-life situation, and the capping efficiency of thicker layer remains undoubtedly better.

These passivated samples were cut into several pieces, and some samples with CdTe- and ZnS-passivation layers were baked at 100°C in vacuum for 12 h. In addition, a ZnS-coated sample was baked at 100°C for 4 h in air. Baking in air at 100°C for 4 h was done to simulate the cumulative baking of wafers in the successive photolithography steps during device fabrication. The XPS spectra were obtained using Al $K_\alpha$ radiation ($h\nu = 1{,}486.6$ eV). The experimental resolution was 0.8 eV. The spectra of Hg 4f, Cd 3d, Te 3d, Zn 2p, S 2p, O 1s, and C 1s were recorded. The shifts caused by the charging effect were taken care of by using the C 1s peak at 284.6 eV as a reference. The HgCdTe compositions were calculated from the areas under the spectrum lines and using atomic-sensitivity factors 3.15, 3.5, 5.4, 4.8, and 0.54 for Hg, Cd, Te, Zn, and S, respectively. The measurements were performed on baked and as-deposited samples as a function of depth, with each etching step done in situ by ion milling. Sample temperature was maintained at 13°C during measurements to control heating-induced artifacts. Baking of all the samples have been carried out in situ just after the completion of deposition, except for one sample, which was baked in air.

## RESULTS AND DISCUSSION

### CdTe/$Hg_{1-x}Cd_xTe$

Figure 1 shows integrated intensities of Hg 4f core-level peaks of the prebaked and vacuum-baked samples at various depths. The integrated intensities of Cd 3d core-level peaks of the prebaked and vacuum-baked samples are shown in Fig. 2. The Te 3d core-level spectra of prebaked and vacuum-baked samples are shown in Fig. 3a and b, respectively. As mentioned in the previous section, the thickness of the CdTe layer is 200 Å. It is quite evident from Fig. 1 that, even in the prebaked case, Hg has diffused in the CdTe matrix. The Hg signal can be seen from a depth of approximately 120 Å from the surface. It means Hg has out-diffused an approximate depth of 80 Å toward the surface from the "original" interface. The integrated intensities of Cd 3d peaks show a decrease (expect for the top level, i.e., surface) as we go toward the MCT substrate. Initially, it shows a decrease in intensity (from 150 Å to 400 Å), and then, it becomes more or less constant. The higher intensity close to the surface is due to a higher concentration of Cd, as we have deposited CdTe on MCT. However, as Hg has diffused into the CdTe matrix to an appreciable depth, a substantial part of the CdTe matrix has practically become HgCdTe. It is to be noted that the depth up to

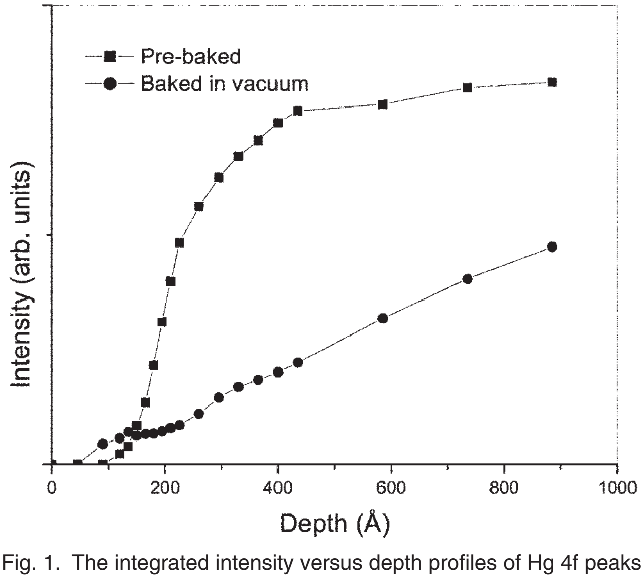

Fig. 1. The integrated intensity versus depth profiles of Hg 4f peaks of prebaked and vacuum-baked CdTe/HgCdTe samples.

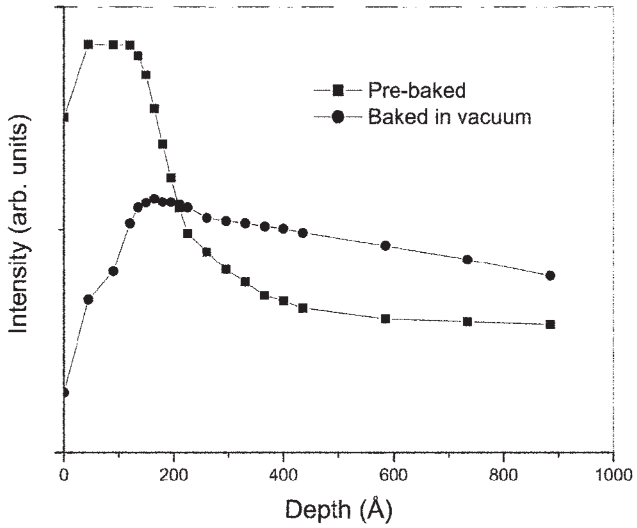

Fig. 2. The integrated intensity versus depth profiles of Cd 3d peaks of prebaked and vacuum-baked CdTe/HgCdTe samples.

which Hg has diffused, it has most likely gone to Cd sites. Similarly, Cd has gone into the HgCdTe matrix at Hg sites. This can be seen from the opposite trend of intensity profiles in the two cases (Figs. 1 and 2), i.e., the intensity of Hg 4f core levels is decreasing as one approaches the surface, whereas the intensity of Cd 3d core level increases. Also from Fig. 3a, it can be seen that except at the surface, contrary to Hg and Cd core levels, Te 3d core-level spectra do not show any significant change in intensity up to the tested depth of 885 Å. At the surface, a clear signature of the formation of tellurium oxide can be seen, as indicated by the peak appearing at 576.3 eV.

Now, we turn our attention to the case in which the passivated sample (CdTe/MCT) was baked at 100°C in vacuum for 12 h. From Fig. 1, it is clear that the absolute intensity of the Hg core levels have reduced considerably. The Hg signal is observed right from the surface, indicating more outward diffusion of Hg. The reduction of the Hg signal and its presence at the surface strongly suggest loss of Hg from the sample. This loss was found to be much more pronounced from the interfacial region. As compared to the prebaked case, we observe that Cd is now more uniformly distributed in the MCT matrix, i.e., from the interface of CdTe and MCT to the tested depth of 885 Å (Fig. 2). Also, Fig. 2 suggests that Cd has diffused inside the MCT matrix from the CdTe-passivating layer. This results in a decrease in its signal until the interface (~200 Å) and an enhancement of its signal at higher depths. However, the present measurements cannot rule out the possibility of some loss of Cd from the sample. Unlike the prebaked case, on baking in vacuum, the intensity profile is not totally opposite to that of Hg. It seems that with more outward diffusion of Hg on vacuum baking, Cd has replaced it, diffusing in from the top and, maybe, was also lost from the sample. A comparison of Fig. 3a and b shows a slight reduction in the intensity of the Te core-level line. This suggests that on baking, Te is also lost from the sample, but no change in its intensity profile suggests that the position of Te atoms in the entire sample matrix remains as it was in the prebaked case.

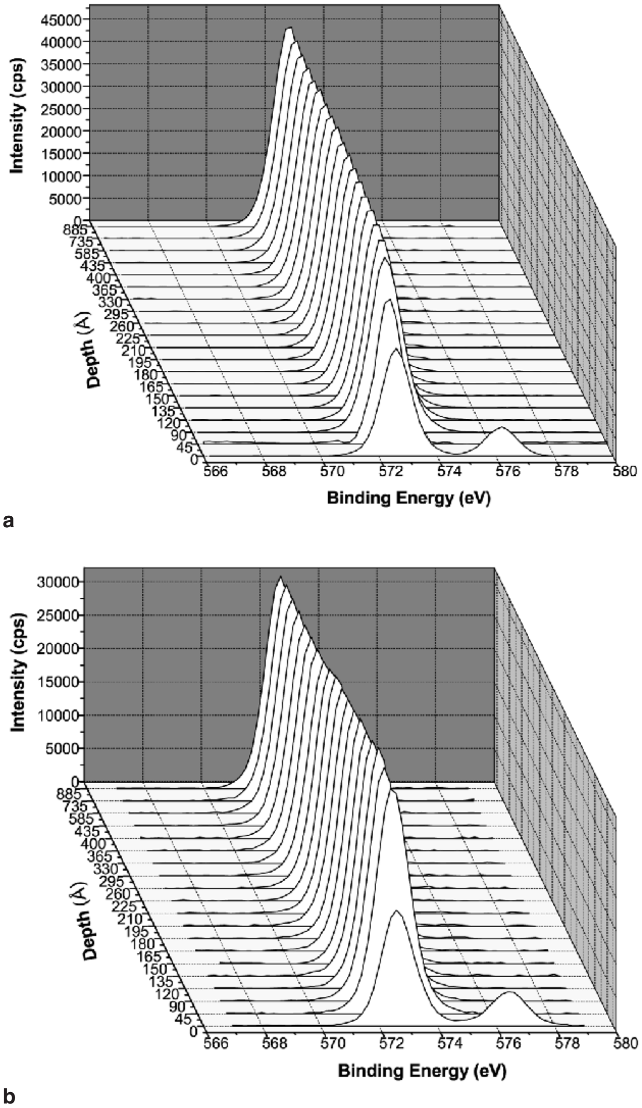

Fig. 3. The Te $3d_{5/2}$ spectra of (a) prebaked and (b) vacuum-baked CdTe/HgCdTe samples as a function of depth.

To quantify our data, we have calculated layer composition at various depths (Table I). The relative concentrations of Hg and Cd at various depths were calculated by using similar XPS data of a pure $Hg_{0.8}Cd_{0.2}Te$ epilayer as a reference. It was extremely important to minimize the effect of sputtering. Atomic-concentration profiles of Hg, Cd, and Te were generated using Hg 4f, Cd 3d, and Te 3d core-level data at various depths. It is clear from the atomic concentration versus depth curves (shown in Fig. 4) for $Hg_{0.8}Cd_{0.2}Te$ that, because of sputtering effects, we did not get the actual $Hg_{0.8}Cd_{0.2}Te$ composition in the sample, except on the surface where the atomic concentrations of Cd and Hg were found to be in the ratio of 1:4. On the other hand, x was found out to be 0.2 by Fourier-transform IR spectroscopy

**Table I. Concentrations of Various Constituents of HgCdTe as a Function of Depth in the Prebaked and Vacuum-Baked CdTe/$Hg_{1-x}Cd_xTe$ Samples**

| | CdTe/MCT (Prebaked) | | | CdTe/MCT (Baked in Vacuum) | | |
|---|---|---|---|---|---|---|
| Depth (Å) | Hg | Cd | Te | Hg | Cd | Te |
| 250 | 0.65 | 0.35 | 1 | 0.25 | 0.75 | 1.05 |
| 300 | 0.71 | 0.29 | 1 | 0.31 | 0.69 | 1.03 |
| 350 | 0.76 | 0.24 | 1 | 0.37 | 0.63 | 1.02 |
| 400 | 0.79 | 0.21 | 1 | 0.40 | 0.60 | 1.02 |
| 450 | 0.80 | 0.20 | 1 | 0.43 | 0.57 | 1.01 |
| 500 | 0.80 | 0.20 | 1 | 0.47 | 0.53 | 1.01 |
| 550 | 0.80 | 0.20 | 1 | 0.50 | 0.50 | 1.00 |
| 600 | 0.80 | 0.20 | 1.01 | 0.53 | 0.47 | 0.9 |
| 650 | 0.81 | 0.19 | 1.01 | 0.56 | 0.44 | 0.99 |
| 700 | 0.82 | 0.18 | 1.02 | 0.59 | 0.41 | 0.99 |

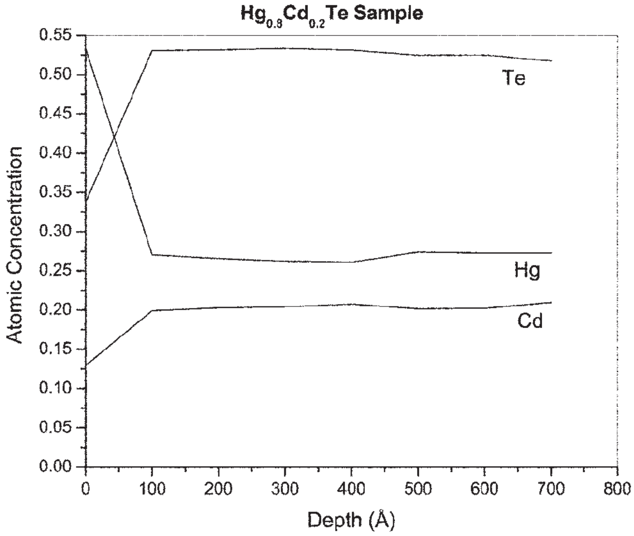

Fig. 4. The atomic-concentration profiles of various constituents of the pure $Hg_{0.8}Cd_{0.2}Te$ sample, used for calibration purpose. Details are described in the text.

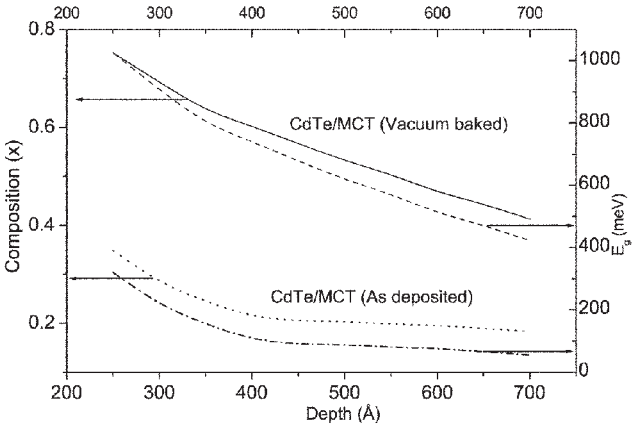

Fig. 5. The variation of x and bandgap (Eg) as a function of depth of prebaked and vacuum-baked CdTe/HgCdTe samples.

measurements. Therefore, to minimize sputtering effects, first, we normalized the atomic concentration of Hg and Cd at various depths to that at the surface for the pure $Hg_{0.8}Cd_{0.2}Te$ sample; after that, we used the same normalization factors at corresponding depths to normalize their atomic concentrations in other samples. Results are given in Table I, and it is clear that the outcome is quite satisfactory, showing approximately $x = 0.2$ below a depth of ~400 Å. However, it should be noted that we could not use the same procedure to normalize Te in pure $Hg_{0.8}Cd_{0.2}Te$, as Te gets converted to its oxide in the top few layers. Because the atomic concentration of Te was calculated without taking its oxide peak into account, it is quite low at the surface as compared to the actual concentration of Te. Therefore, we normalized Te in all samples directly by the value of atomic concentration of Te at corresponding depths. It is clear from the table that actual concentrations of Hg and Cd were achieved, in the case of prebaked sample, above the depth of approximately 400 Å. The higher concentration of Cd in the vacuum-baked sample is due to in-diffusion of Cd from the passivant layer, which is replacing out-diffusing Hg in the sample.

The formation of a graded structure in the case of CdTe/MCT has its obvious advantages, as diffusion of Hg in the CdTe matrix results in a HgCdTe matrix. Figure 5 shows the variation of x and the bandgap ($E_g$) as a function of depth in CdTe/HgCdTe sample. The bandgap was calculated using a relation by Hansen and Schmit.[11] One can clearly see that even in the case of as-deposited sample, the interlayer mixing results in a bandgap gradation from 320 meV close to the surface to 100 meV at a depth of 400 Å. Annealing treatments in the present study have resulted in doubling the energy barrier as well as widening of this high-bandgap layer. An energy barrier to the excess carriers, formed during baking of CdTe/HgCdTe, results in producing a barrier to the excess carriers, thereby leading to reduction in surface-recombination velocity[12] and surface-leakage currents in photodiodes.[5,10]

## ZnS/$Hg_{1-x}Cd_xTe$

Figure 6 shows integrated intensities of Hg 4f core-level peaks recorded at different depths for prebaked, after baking in air for 4 h at 100°C, and after baking in vacuum for 12 h at 100°C. Similar to CdTe/MCT, Hg has diffused into the ZnS matrix. The first signal observed for Hg is at a depth of approximately 170 Å from the surface. In case of CdTe/MCT, Hg was first observed at 120 Å from the surface. This may be due to the fact that unlike diffusion of Hg in ZnS, diffusion of Hg in the CdTe matrix results in the formation of HgCdTe, which is a stable compound. It can be seen from Figs. 7 and 8a, showing the Cd 3d intensity profile and Te $3d_{5/2}$ spectra, that Cd and Te have also diffused into the ZnS matrix up to the same depth as Hg. This is contrary to the CdTe/MCT case in which the concentration profile of Cd was opposite to that of Hg (i.e., Cd was diffusing to vacant Hg sites) and hardly any change was seen in the Te-concentration profile. It was expected; as in case of CdTe/MCT, we had both Cd and

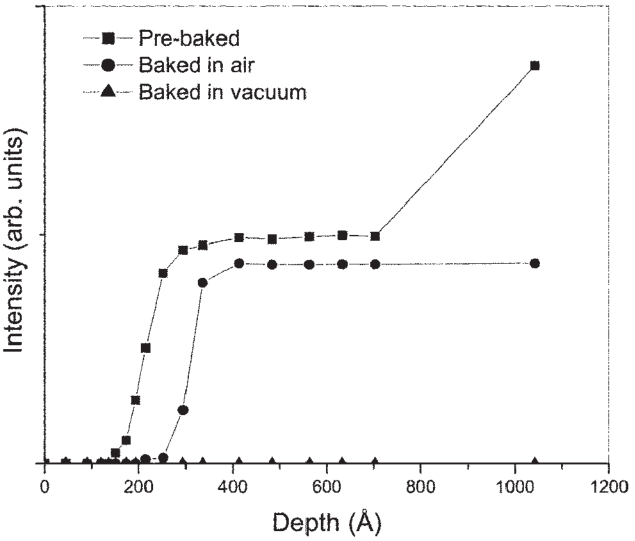

Fig. 6. The integrated intensity versus depth profiles of Hg 4f peaks of prebaked, air-baked, and vacuum-baked ZnS/HgCdTe samples.

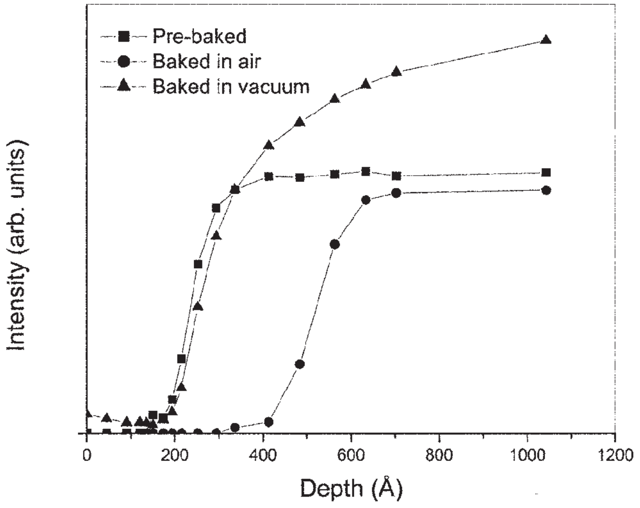

Fig. 7. The integrated intensity versus depth profiles of Cd 3d peaks of prebaked, air-baked, and vacuum-baked ZnS/HgCdTe samples.

Te already present in the passivating layer itself, while in ZnS/MCT, there is no Te or Cd in the passivating layer; therefore, we cannot expect the same kind of intensity profile for Cd and Te here. Also, there is an indication of the formation of tellurium oxide (feature around 576.3 eV) right from the surface to 173 Å. It indicates that the small concentration of Te, which, has diffused up to the surface has been converted into an oxide. The Zn 2p and S 2p spectra (Figs. 9 and 10a) clearly indicate the presence of Zn and S up to the depth of approximately 300 Å and 252 Å, respectively. This suggests a slight diffusion of S and Zn (as the ZnS layer was 200-Å thick) in the MCT matrix. The feature (indicated by an arrow in Fig. 10a) emerging at around 169 eV corresponds to the Te 4s core level. This not only proves slight diffusion of S into MCT matrix but also reflects the reliability of depth determination in the present work.

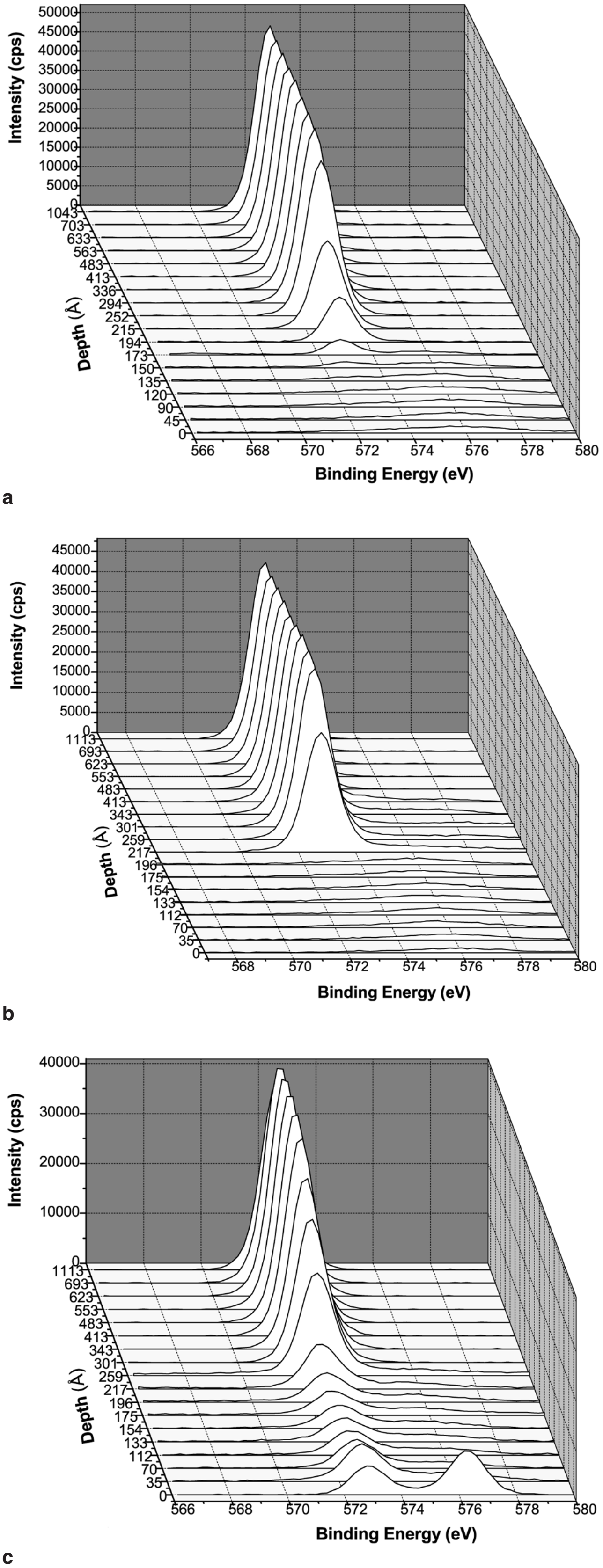

Fig. 8. The Te $3d_{5/2}$ spectra of (a) prebaked, (b) air-baked, and (c) vacuum-baked ZnS/HgCdTe samples as a function of depth.

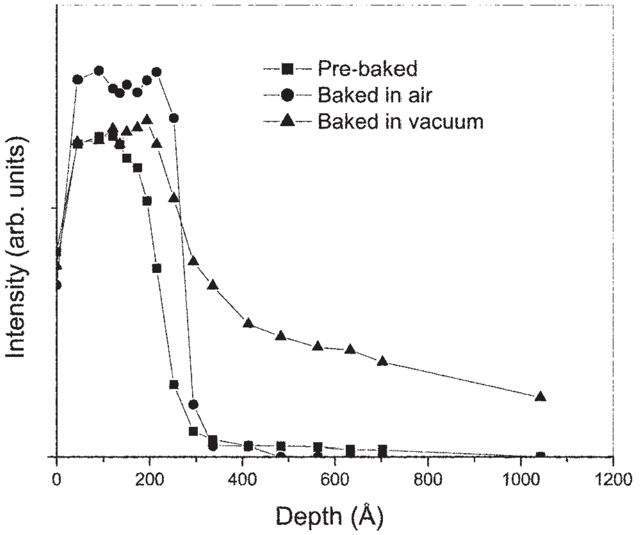

Fig. 9. The integrated intensity versus depth profiles of Zn 2p peaks of prebaked, air-baked, and vacuum-baked ZnS/HgCdTe samples.

Now, we look at the sample baked in air at 100°C for 4 h. No signal of Hg could be seen approximately up to the depth of approximately 250 Å from the surface (Fig. 6). However, comparing the intensity of the Hg signal with the prebaked sample shows a slight decrease, thereby suggesting loss of Hg predominantly from the top layers. The intensity profile of Cd core-level peaks (Fig. 7) shows no signal until ~420 Å. This suggests that Cd is also lost after baking the sample in air at 100°C. The Te $3d_{5/2}$ spectra (Fig. 8b) show a signal at approximately 217 Å. As mentioned earlier, in the prebaked case, the Te signal could be seen at around 173 Å from the surface. Also, one could see a feature at around 576 eV in the spectra of the top levels, indicating the presence of tellurium oxide. It should be noted that because a clear Te signal is detected at 217 Å from the surface, one might infer that the Te loss or conversion into oxide was mainly coming from the ZnS matrix. This is expected, as Te diffused into the ZnS matrix does not have a strong bonding with the surrounding environment as it has in the MCT matrix. As far as the Zn 2p intensity profile is concerned (Fig. 9), the Zn signal was detected from the surface to a depth of ~300 Å. This is the same as the prebaked case. Similar to Zn, no further diffusion of S in the MCT matrix was observed. This can be understood from the fact that, in air baking, oxygen (in the form of a tellurium-oxide barrier layer) might have filled all channels created by Hg, Cd, and Te out-diffusion, thereby blocking Zn and S from diffusing further into the MCT matrix.

Baking the ZnS/MCT sample in vacuum for 12 h at 100°C results in complete loss of Hg. No trace of Hg up to the tested depth of more than 1,000 Å was detected. The Cd 3d signal (Fig. 7) could be detected right from the surface. However, an appreciable signal is detected approximately from the interface of ZnS/MCT, i.e., ~200 Å. The absolute intensity of

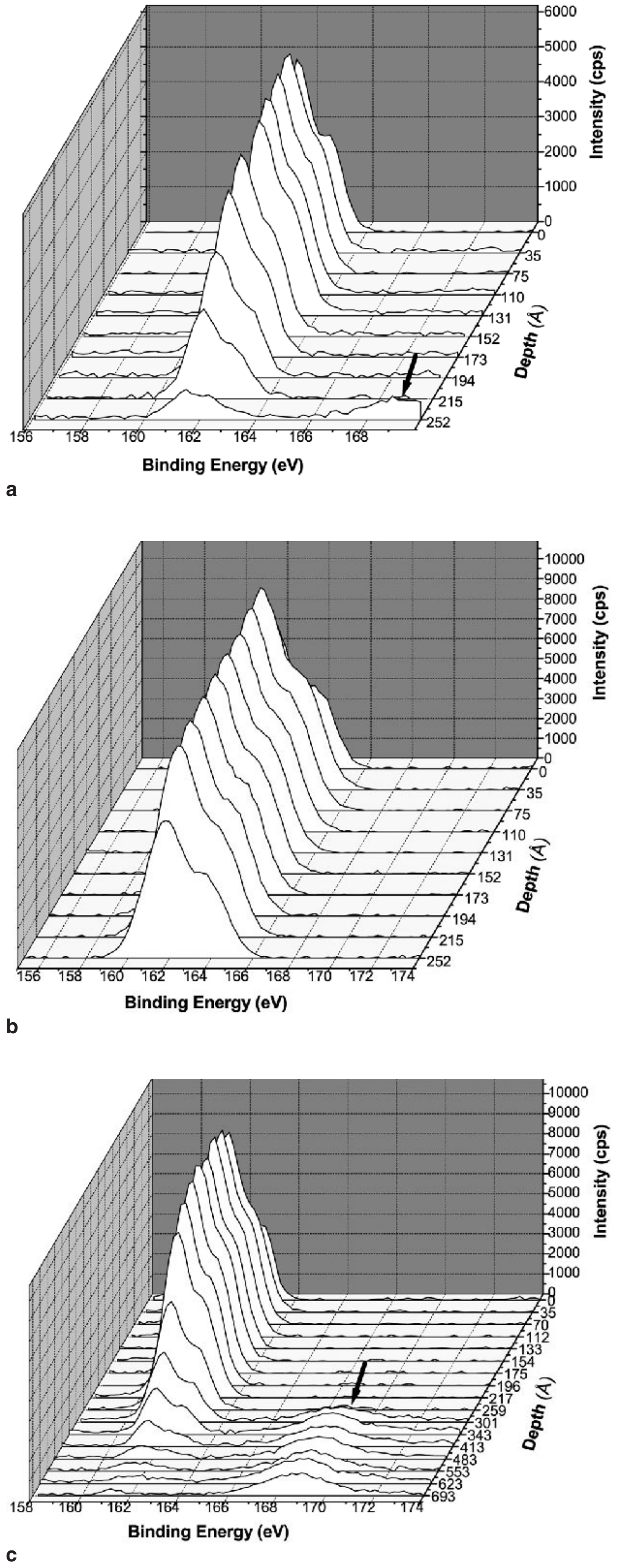

Fig. 10. The S 2p spectra of (a) prebaked, (b) air-baked, and (c) vacuum-baked ZnS/HgCdTe samples as a function of depth. The Te 4s peak/feature is indicated by an arrow.

Cd 3d core-level peaks of the prebaked sample is slightly higher than the samples baked in air. Comparison of the three cases (Fig. 7) suggests that Cd is lost until the depth of approximately 500 Å on air baking. In comparison to the prebaked sample, in the case of the vacuum-baked sample, the intensity of the Cd 3d peak is finite until the surface, which suggests outward diffusion. However, the increase in intensity after baking in vacuum is much more pronounced from the depth of 200 Å onward, showing the diffusion of Cd from the passivating layer to the MCT matrix. This may be because of the fact that because Hg has diffused out, vacant sites are available in the MCT matrix for diffusion of Cd. The Te signal (Fig. 8c) can be seen right from the top to the tested depth of 1,113 Å. The concentration gradient is much different from that of the air-baked sample, and Te has clearly diffused into the ZnS matrix. The absolute intensities in Fig. 8a–c suggest that the diffusion of Te takes place from the interface to the ZnS matrix. A clear formation of a tellurium-oxide peak (at approximately 576.3 eV) and its existence up to the depth of 259 Å can be seen. This is also reflected in the S 2p spectra (Fig. 10c), which clearly show the presence of a Te 4s level along with S 2p core levels. However, both Zn and S have diffused into the MCT matrix, at least up to the tested depth of approximately 1,000 Å (Figs. 9 and 10c). It seems that in vacuum baking, initially, a slight out-diffusion of Zn and S takes place. This results in nonstoichiometric ZnS on top. The vacancies left behind in the passivation layer created an effective channel for Hg, Cd, and Te to out-diffuse. The Hg totally disappears from the sample, as it is known to be less strongly bonded than the other constituents. This, in turn, creates a channel for Zn and S in-diffusion. This result indicates bake instability of ZnS as a passivation layer.

## SUMMARY

We have carried out a detailed XPS study to examine the bake stability of ZnS and CdTe on HgCdTe. The present work suggests that as a single passivation layer, neither CdTe nor ZnS are suitable. Because of less compatibility of ZnS and MCT in the prebaked and air-baked cases, diffusion of Hg, Cd, and Te into the ZnS matrix and of Zn and S into the MCT matrix is less compared to CdTe on MCT. Vacuum baking has a very detrimental effect in the case of ZnS/MCT, as all Hg is lost from the MCT matrix. Baking of CdTe/HgCdTe wafers leads to compositional grading in the surface layer, which moves the CdTe/HgCdTe electrical interface deeper into the defect-free region and, hence, is desirable. It is, therefore, concluded that an appropriate post-deposition annealing treatment (preferably in the deposition chamber itself) should precede the device fabrication and packaging. Such a treatment will be helpful in producing a cleaner and more stable interface and, hence, will result in long-term stability of detector performance. However, the conversion of a part of the CdTe layer into HgCdTe, caused by interlayer mixing, necessitates its encapsulation by another dielectric layer. Because this study indicates the instability of ZnS film under the harsh environment of packaging, the use of $Si_3N_4$ for encapsulation of CdTe/HgCdTe may be explored.

## ACKNOWLEDGEMENTS

Financial support from the Department of Science and Technology, New Delhi, India, is gratefully acknowledged. One of us (RP) is grateful to the University of South Australia for financial support to carry out XPS measurements. One of the authors (Anjali) is very grateful to the Council of Scientific & Industrial Research, New Delhi, India, for the Junior Research Fellowship.

## REFERENCES

1. Y. Nemirovsky and I. Bloom, *Infrared Phys.* 27, 143 (1987).
2. Y. Nemirovsky, N. Manizer, and E. Weiss, *Properties of Narrow Gap Cadmium Based Compounds,* ed. P. Capper (London: INSPEC, 1994), p. 284.
3. O.P. Agnihotri, C.A. Musca, and L. Faraone, *Semicond. Sci. Technol.* 13, 839 (1998).
4. A.F. Tasch, Jr., R.A. Chapman, and B.H. Breazeale, *J. Appl. Phys.* 41, 4202 (1970).
5. J.K. White, J. Antoszwski, R. Pal, C.A. Musca, J.M. Dell, L. Faraone, and J. Pitrowski, *J. Electron. Mater.* 31, 743 (2002).
6. G. Sarusi, G. Cinadar, A. Zemel, D. Eger, and Y. Shapira, *J. Appl. Phys.* 71, 5070 (1992).
7. L.O. Bubulac, W.E. Tennant, J. Bajaj, J. Sheng, R. Brigham, A.H.B. Vanderwyck, M. Zandian, and W.V. McLevige, *J. Electron. Mater.* 24, 1175 (1995).
8. O.P. Agnihotri, H.K. Sehgal, R. Pal, and V. Gopal, *Appl. Phys. Lett.* 77, 1330 (2000).
9. J.M. Dell, J. Antoszwski, J.K. White, R. Pal, T. Nguyen, C.A. Musca, and L. Faraone, *Proc. SPIE* 44, 54 (2001).
10. S.Y. An, J.S. Kim, D.W. Seo, and S.H. Suh, *J. Electron. Mater.* 31, 683 (2002).
11. G.L. Hansen and J.L. Schmit, *J. Appl. Phys.* 54, 1639 (1983).
12. R. Pal, V. Gopal, P.K. Chaudhury, B.L. Sharma, P.K. Basu, O.P. Agnihotri, and V. Kumar, *J. Electron. Mater.* 31, 103 (2001).